Basal Area and Biomass Estimates of Loblolly Pine Stands Using L-band UAVSAR

William L. Marks, John S. Iiames, Ross S. Lunetta, Siamak Khorram, and Thomas H. Mace

Abstract

Fully polarimetric L-band Synthetic Aperture Radar (SAR) backscatter was collected using NASA's Unmanned Aerial Vehicle (UAV) SAR and regressed with in situ measurements of basal area (BA) and above ground biomass (AGB) of mature loblolly pine stands in North Carolina. Results found HH polarization consistently displayed the lowest correlations where HV and VV exhibited the highest correlations in all groups for both BA and AGB. When plantation stands were analyzed separately (plantation versus natural), correlation improved significantly for both BA (R^2 = 0.65, HV) and AGB (R^2 = 0.66, VV). Similarly, results improved when natural stands were analyzed separately resulting in the highest correlation for AGB (R^2 = 0.63, HV and VV). Data decomposition using the Freeman 3-component model indicated that the relative low correlations were due to the saturation of the L-band backscatter across the majority of the study area.

Introduction

The derivation of forest biophysical factors using remote sensing approaches has the potential to minimize requirements for labor intensive, ground-based estimates and facilitate the generation of data sets across extended geographic areas. The objective of this study was to assess the relationship of high resolution fully polarimetric L-band Synthetic Aperture Radar (SAR) backscatter collected using NASA's Unmanned Aerial Vehicle (UAV) SAR with *in situ* measurements of basal area (BA) and above ground biomass (AGB) of mature loblolly pine stands using simple linear regression.

UAV platforms with optical or lidar sensors have been especially useful in addressing optimal spatial and spectral resolutions and repeat cycles in the acquisition of environmental data (Berni *et al.*, 2009). For example, the assessment of forest biophysical parameters utilizing UAV platforms have been demonstrated for estimating canopy structure by extracting three-dimensional canopy surfaces from high resolution two-dimensional imagery (Dandois and Ellis, 2010). Leaf area index (LAI), chlorophyll content, water stress detection, and canopy temperature have been estimated indirectly using a helicopter UAV mounted with a thermal and hyperspectral optical sensor (Zarco-Tejada *et al.*, 2009). The benefits of employing a UAV SAR system for the study of forest biomass include: (a) counteracting the difficulties of wind gusts and turbulence in flying the same pass on multiple occasions, and (b) maintaining antennae angle despite differing yaw angles created by cross-wind issues (Rosen *et al.*, 2006). The ability to maintain aerial track and antennae pointing capabilities warrant the use of these controlled flight management systems (Rosen *et al.*, 2006).

Factors affecting forest AGB estimation from radar backscatter include forest structure (size and age class, stand density, branch angular patterns), site characteristics (slope, aspect, soil moisture content), dialectric constant (plant water content and specific gravity), radar measurement geometry patterns (incidence angle and spatial resolution), and radar bandwidth (Robinson *et al.*, 2013). Specific to loblolly pine forest structure, leaf biomass accumulation also varies inter-annually by producing two to three needles flushes throughout the growing season, with maximum leaf biomass (i.e., LAI) occurring in August (Dewey *et al.*, 2006). Site characteristics such as fertility and drought also affect loblolly pine canopy architecture indicated by significant variation in indeterminate growth (multiple flushes) and high plasticity (i.e., developmental patterns) in foliage accretion and abscission (Sampson *et al.*, 2003; Iiames *et al.*, 2008).

Past SAR studies have used L-band radar preferentially over shorter wavelength (i.e., C-band or X-band) systems to maximize above ground biomass (AGB) sensitivity (Imhoff *et al.*, 1998). A study by Wu and Sader (1987) examined correlations on 18 forested plots with fully polarimetric NASA AIRSAR (L-band) backscatter to derive vegetative parameter data for natural pine, bottomland hardwood, and swamp forest with deciduous understory across the southern US Gulf Plain physiographic region. Wu and Sader (1987) documented the potential application of SAR to quantify vegetation characteristics including total-tree biomass, basal area (BA), and tree height. Past research has focused on establishing correlations between tree height, BA, and AGB using backscatter responses from single polarizations and polarization ratios. Results from linear regression analysis have determined that the best correlations were achieved with the VH channel, with all three polarizations ranging from (R^2 = 0.50 to 0.82) for BA, (R^2 = 0.45 to 0.52) for tree height, and (R^2 = 0.74 to 0.89) for AGB (Wu and Sader, 1987). Additionally, the HV channel dominated canopy

John S. Iiames and Ross S. Lunetta are with the United States Environmental Protection Agency, 109 T.W. Alexander Dr., MD E243-05, Research Triangle Park, North Carolina 27711 (iiames.john@epa.gov).

William L. Marks and Siamak Khorram are with North Carolina State University, Department of Forestry and Environmental Resources, Box 7106, Raleigh, NC 27695.

Thomas H. Mace is with the U.S. National Aeronautics and Space Administration, Office of the Associate Director for Operations, Dryden Flight Research Center, Edwards, CA 93523.

Photogrammetric Engineering & Remote Sensing
Vol. 80, No. 1, January 2014, pp. 33–42.

0099-1112/14/8001–33/$3.00/0

doi: 10.14358/PERS.80.1.33

scattering when compared to the VV and HH channels (Wu and Sader, 1987).

Kasischke *et al.* (1995) examined the relationship between SAR backscatter and AGB in 61 loblolly pine stands aged 1 to 100 years at the Duke Forest near Durham, North Carolina using NASA's AIRSAR. They found high correlations (R^2 = 0.95) for total branch AGB using L-band HV in stands with AGB between 2 to 39 Mg ha^{-1}. These results indicated a high potential for modeling loblolly pine in the Piedmont region of North Carolina in stands of low biomass. A study by Stellingwerf and Hussin (1997) found high correlations between L-band backscatter and forest parameters (i.e., age [R^2 = 0.93 HV], DBH [R^2 = 0.94 HV], BA [R^2 = 0.90 HV], height [R^2 = 0.83 HV], cords/acre [R^2 = 0.91 HV], trees/acre [R^2 = 0.81 HV]) in young (4 to 17 years) slash pine stands, but low correlations with older (16 to 53 years) stands (i.e., age [R^2 = 0.47 VV], DBH [R^2 = 0.22 VH], BA [R^2 = 0.40 HV], height [R^2 = 0.11 HH], cords/acre [R^2 = 0.47 HV], trees/acre [R^2 = 0.15 HH]). In general, data sets with the V-polarization (VV, HV, VH) produced the highest correlations with respect to these stand parameters. This was credited to the strong coupling between the vertical forest structure and the V-polarized radar waves. The cross-polarized radar waves (VH or HV) performed better than the VV-polarization due to depolarization issues with the returning vertical signal from the VV-polarization. They attributed the success with young stands to lower variability between sample sites, whereas the older stands had variability artificially introduced due to varying forest management practices. Dobson, *et al.* (1992) indicated that HV (R^2 = 0.96) backscatter best characterized AGB compared to HH (R^2 = 0.89) or VV (R^2 = 0.92). However, Wu (1987) found the strongest correlation (R^2 = 0.89) using the VV channel when estimating AGB of plantation stands of slash pine in the US gulf coast using the JPL AIRSAR. The L-band (λ = 25 cm) has been shown to better characterize woody stem structure compared to shorter wavelength radar which are better suited for characterizing the vegetation in the canopy (Waring *et al.*, 1995). The relationship between size of the scattering mechanism and wavelength is responsible for the greater canopy penetration and subsequent returns using L-band radar (Dobson, 2000).

The culmination of numerous studies has shown that backscatter saturates, becoming unresponsive once AGB approaches 60 to 100 Mg ha^{-1} in loblolly pine (Dobson *et al.*, 1992; Rauste *et al.*, 1994) or BA beyond certain thresholds (Dobson *et al.*, 1992; Kasischke, *et al.*, 1995). Imhoff (1993 and 1995) and Wang *et al.* (2006) determined that L-band backscatter was largely saturated at 40 Mg ha^{-1} and Lucas *et al.* (2000) placed L-band saturation at approximately 60 to 80 Mg ha^{-1}. L-band radar, while more accurate for estimating AGB than C-band or X-band radar, reaches saturation at lower levels than P-band (Kasischke, *et al.*, 1995).

In this study, full polarimetric L-band data using NASA Jet Propulsion Laboratory's (JPL's) Uninhabited Aerial Vehicle Synthetic Aperture Radar (UAVSAR) was flown at a global average GPS altitude of 12,536 meters above mean sea level (MSL) in the coastal plain of North Carolina. The study objective was to evaluate the feasibility of using high spatial resolution (6.0 m) L-band radar data to characterize BA and AGB in loblolly pine. Prior studies used varying spatial resolution data including 3.0 m (Wang *et al.*, 2006), 10.98 m (Wu and Sader, 1987; Wu, 1987; Rauste *et al.*, 1994); 12.1 × 6.7 m (Kasischke *et al.*, 1995); and 12 m × 7 m (Imhoff, 1995). Higher spatial resolution SAR data has the advantage of providing more data points, yet also may increase speckle noise thereby reducing quality (Robinson *et al.*, 2013). A major goal was to assess the differential in performance associated with the high resolution HH, VV, HV channels to characterize the BA and AGB of mature loblolly pine (*Pinus taeda)* stands. While airborne SAR has been used to varying degrees of success in many previous forest characterization studies, this study assesses feasibility in the North Carolina coastal plain, a unique ecosystem consisting of riverine and palustrine (e.g., Pocosins) wetland systems, where soil types vary from sandy loams to rich organic soils.

Study Area

UAVSAR data were collected on 13 August 2009 along a northwest-to-southeast rectangular flight swath (180 km × 21 km) within the Neuse River Basin (NRB) of North Carolina. The flight line was located between Wilson, North Carolina in the northwest to Cape Lookout in the southeast (Figure 1). The coastal plain region comprises approximately 45 percent of the land area in North Carolina. The region is characterized by low-lying, relatively flat terrain with sandy soils. The majority of North Carolina's wetland areas are present within this region (Orr and Stuart, 2000). The area is dominated by natural pine, bottomland hardwood, and swamp forest with deciduous understory present at most locations. Study area loblolly stands ranged from 10 to 50 m^2 ha^{-1} of BA and 65 to 265 Mg ha^{-1} of AGB.

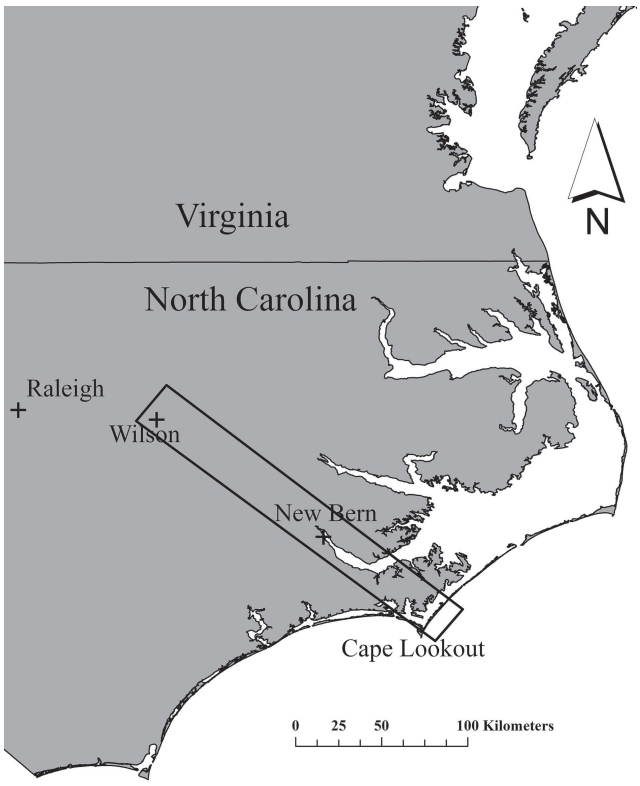

Figure 1. UAVSAR North Carolina study area denoted by rectangular (180 m × 21 m) swath within the Neuse River Basin. Data were collected on 13 August 2009 at a global average altitude of 12,536 m ASL.

Methods

Both natural and plantation stands of loblolly pine were selected to represent the dominate species type in North Carolina southeastern coastal plain by wood volume (NCFS, 2010). Field data measurements were made at 24 randomly selected sample sites located throughout the flight line (3,780 km^2). UAVSAR analyses were performed on four forest stand types including (a) natural and plantation stands combined (AS), (b) only natural stands (NS), (c) only plantation stands (PS), and (d) plantation stands thinned (PS-T). Each set was separately analyzed for BA and AGB elements (n = 6). The relationship between backscatter (sigma°) and field measurements was assessed using simple linear regression. The levels of correlation found in the different combinations of polarizations and stand-type samples were used to determine the utility of L-band UAVSAR data to assess BA and AGB in the North Carolina coastal plain.

UAVSAR Data

The polarimetric L-band radar system was pod-mounted on the underside of the NASA Gulfstream III aircraft. UAVSAR data were collected at a near range look angle of 20° and far range look angle of 65.2° on 13 August 2009, along a 312.39° heading at 12,563 m (MSL). Significant precipitation occurred in the southeastern third of the collection swath on 12 August 2009 with Beaufort (47.0 mm) and Havelock (111.7 mm) receiving the greatest amounts. The remainder of the swath received nominal precipitation amounts (New Bern = 8.6 mm; Wilson = 2.8 mm). Additionally, trace amounts of precipitation fell throughout the swath on 13 August 13 with the southeastern third, again receiving the most precipitation (New Bern = 4.4 mm and Beaufort = 18.3 mm). This dataset was collected in multi-looked polarimetric (HH, VV, HV) mode, orthorectified, and provided in a Esri GRD (Esri, 2013) format in an equiangular geographic coordinate system (longitude and latitude) with a postprocessed pixel resolution of 6.0 m. The fourth channel, VH, was excluded due to the reciprocal nature of electromagnetic wave scattering, meaning that HV and VH backscatter data are identical (Wu and Sader, 1987). Within each pixel, there were twelve azimuth and three range looks for a total of 36 "looks" per pixel. Accordingly, the sensor measured the returns from 36 "looks" for each pixel during a single sweep and calculated the average in order to reduce speckle noise in the final product (Franceschetti and Lanari, 1999). Linear power units (watts) were converted to decibel units (sigma°) to measure returned backscatter intensity (NASA JPL, 2011). The data were converted to an image (.img) file format for compatibility with ERDAS Imagine® software (ERDAS, 2010).

Field Measurements

Field measurement data were collected at the 24 loblolly pine sample plots throughout the UAVSAR swath within the NRB during late-January to early-February 2011. These 24 plots were nearly evenly distributed between planted (n = 13) and natural (n = 11) stands of mature loblolly pine. All 24 plots were located within the 40° to 60.2° incident angle range throughout the swath. Despite the 18-month time differential between the UAVSAR collect and the field measurements, only one growing season separated these two data collects. Error attributed to the time differential was considered to be minimal given the maturity of the loblolly stands. Loblolly mean annual increment growth increases at a decreasing rate by age 15, and growth asymptotes at age 35 (Coble, 2009). A stratified random sampling scheme based on forest type classification was applied to select the locations for field measurements. The swath was first subset into smaller 10.5 km × 10.5 km units and evergreen forests were isolated for sampling using the NLCD 2006 land-cover data. Hawth's Tools (Beyer, 2004), an application for use with ArcMap®, was then used to generate random points within each section. An oversampling was incorporated into the design to facilitate additional refinement. Due to site access issues, sample sites were chosen in the general vicinity (i.e., next available access) of the initially randomly stratified locations. This type of "purposive" sampling can affect statements of accuracy and levels of confidence. Operator bias can be minimized by placement of sample sites completely contained within one stand type thereby eliminating boundary issues, and sampling across the spectrum of stand variation (McCoy, 2005).

High-resolution National Agricultural Imagery Program (NAIP) digital aerial imagery (1.0 m) was utilized to search for sample sites prior to field deployments. Potential sample sites were selected based on a number of qualitative criteria including the (a) potential loblolly pine dominated areas, (b) reasonable road accessibility, and (c) stand homogeneity to minimize variability of BA measurements to maximize the extrapolation (representativeness) of field measurement data. The extrapolation potential minimized any minor errors in GPS coordinates or in the georectificaton of the UAVSAR data. For the same reason, the center point of each sample site had to be at least 50 m from other cover types (i.e., roads, agricultural fields, urban areas, and wetlands). This ensured that non-forest areas would not be included in the sampled UAVSAR data. A total of 24 loblolly pine stands were included in the final sample set.

After selecting homogenous forest areas, a center point for each survey was established and recorded using a Garmin GPSMAP 62S GPS receiver. Point sampling methodology was employed to inventory all 24 sites. Point measurements were made using a factor 10 BA factor prism. Species type, crown class (dominant, co-dominant, intermediate, suppressed), and diameter at breast height (DBH) were measured for each sampled tree. From these collected data trees per hectare (TPH) by DBH and BA were calculated (m^2 ha^{-1}). Height measurements were taken for two to three trees per plot in the co-dominant/dominant height class range to establish canopy height at the stand level. Ancillary comments included site condition, and species abundances for each height class range (i.e., understory, intermediate, co-dominant, dominant). Crown closure (CC) estimates were derived from 2010 (leaf-off) three-band DOQQ high-resolution NAIP imagery (0.15 m) using 30.5 m × 30.5 m image segments clipped to individual sample sites (North Carolina OneMap, 2010). These 929 m^2 image segments were then classified in ERDAS Imagine® using an unsupervised algorithm (ISODATA). Crown/no-crown thresholds were applied to these single-band classified images to determine CC percentages assigned to each sample site. Crown closure is defined as the proportion of the forest floor covered by the vertical projection of the tree crowns (Jennings *et al.*, 1999).

Above Ground Biomass Measurements

To extend DBH to height measurements across all trees within each of the 24 plots, tree heights were estimated using a loblolly height-diameter relationship posited by Trincado *et al.* (2006). North Carolina coastal plain loblolly pine heights were regressed against DBH using the following relationship:

$$h = 1.37 + 4.0779\, d^{0.4386} \quad (1)$$

where h is tree height in meters, and d is DBH in centimeters. AGB for individual loblolly pine trees was then modeled using the below equation published by Williams and Gresham (2006):

$$\text{Total Above Ground Biomass (kg)} = 0.0201 d^2 h + 14.995 \quad (2)$$

where h (tree height) is in meters and d (DBH) is in cm. The ABG of the individual sampled trees was then scaled to Mg ha^{-1}, an input variable for each site to support correlation analyses with UAVSAR backscatter data.

UAVSAR Data Processing and Analysis

The mean UAVSAR backscatter intensity values (sigma°) were extracted from each sample location corresponding to three data resolutions (i.e., 3 × 3, 324 m^2; 5 × 5, 900 m^2; and 7 × 7, 1,764 m^2) using ERDAS Model Maker (ERDAS, 2010). We applied this averaging to generate a better estimate of the mean and reduce the variance provided that the spatial pattern remained homogeneous. We first employed a 9 × 9 moving window median filtering process to reduce speckle-noise in the HV polarization to test gains in correlation between filtered and unfiltered data (Wu and Sader, 1987). Sigma° values were regressed against BA (m^2 ha^{-1}) and AGB (Mg ha^{-1}) for all 24 plots, stratified by stand type (i.e., NS or PS), using Microsoft Excel® Data Analysis Tools (Meyer and Avery, 2009).

Beyond correlating dominant decibel (DB) values, we also investigated three derivatives including the depolarization ratio, polarization correlation, and differential reflectivity ratio. Additionally, we also decomposed the UAVSAR data so that each pixel would be classified as one of three representative bounce types (a) single bounce, (b) double bounce, or (c) volumetric scattering. The European Space Agency's PolSAR Pro software package (ESA, 2012) was used to implement the Freeman 3-component decomposition analysis (Freeman and Durden, 1998; Hansch, 2010).

Results and Discussion

Forest Biophysical Measurements

The 24 loblolly pine sample sites were stratified by PS (n = 13) and NS (n = 11) and a summary of the biophysical measurements for each of the sites is shown in Table 1. Within the PS, 10 of 13 sample sites had been thinned, significantly reducing AGB, BA, and CC (Sites 7 to 9). In general, BA, AGB, and CC measurements were higher in the NS than in the PS (Table 2). BA was greatest in the NS ($\overline{X}$ = 36.5 m^2 ha^{-1}, s = 9.1 m^2 ha^{-1}) compared to PS ($\overline{X}$ = 25.6 m^2 ha^{-1}, s = 15.0 m^2 ha^{-1}) and PST ($\overline{X}$ = 17.9 m^2 ha^{-1}, s = 3.7 m^2 ha^{-1}). CC (NS $\overline{X}$ = 66.1%, s = 10.7%; PS $\overline{X}$ = 51.2%, s = 19.1%; PS-T $\overline{X}$ = 42.6%, s = 10.9%) and AGB (NS $\overline{X}$ = 145.2 Mg ha^{-1}, s = 43.9 Mg ha^{-1}; PS $\overline{X}$ = 132.5 Mg ha^{-1}, s = 69.7 Mg ha^{-1}; PS-T $\overline{X}$ = 96.5 Mg ha^{1}, s = 15.5 Mg ha^{-1}) trended similar to BA.

Table 3 documents the regression analysis comparing all PS combinations of AGB, BA, and CC showing good fit among all three biophysical combinations (AGB versus BA, AGB versus CC, and BA versus CC). However, these results are tempered when comparing the regression coefficients and p-values against that of the PS-T. Precipitous coefficient of determination (R^2) drops occurred between AGB and BA for PS (R^2 = 0.97) and PS-T (R^2 = 0.44), AGB and CC for PS (R^2 = 0.81) and PS-T (R^2 = 0.32), and BA and CC for PS (R^2 = 0.73) and PS–T (R^2 = 0.07). The NS showed a good fit between AGB and BA (R^2 = 0.63), but the fit was not significant for other two comparisons (AGB versus CC and BA versus CC).

SAR Data Decomposition

We examined the potential radar saturation issue by analyzing backscattering type. Volumetric scattering within the canopy layer of forests may cause saturation limiting the utility of radar backscatter values to distinguish stem densities (double bounce). In this scenario, radar energy is not penetrating the canopy to accurately characterize the main stems. To explore this concept we decomposed each UAVSAR data pixel into one of three representative bounce types corresponding to (a) single bounce, (b) double bounce, or (c) volumetric scattering (Table 4). Based on the design to extract the simplistic segmentation of bounce types from this imagery and not

Table 1. Summary of Stand Type Types Corresponding to Natural Stand (NS), Plantation Stand (PS), PS-T (Planted Stands - Thinned), Basal Area (BA), and Above Ground Biomass (AGB), across All 24 Sample Sites

Site	Stand Type	BA (m^2 ha^{-1})	AGB (Mg ha^{-1})
1	NS	29.8	65.9
2	NS	36.7	120.0
3	NS	41.3	161.4
4	PS/PS-T	20.7	89.5
5	PS/PS-T	20.7	106.6
6	PS/PS-T	18.4	95.0
7	PS	50.5	248.1
8	PS	52.8	262.3
9	PS	50.5	246.5
10	NS	45.9	197.1
11	NS	45.9	177.3
12	NS	48.2	187.0
13	NS	34.4	165.4
14	NS	34.4	164.6
15	PS/PS-T	16.1	80.4
16	PS/PS-T	16.1	81.7
17	PS/PS-T	18.4	93.5
18	NS	32.1	101.8
19	PS/PS-T	25.3	127.3
20	NS	36.7	169.5
21	NS	16.1	87.2
22	PS/PS-T	16.1	112.7
23	PS/PS-T	11.5	79.3
24	PS/PS-T	16.1	98.8

Table 2. Forest Biophysical Measurements for NS (Natural Stands) PS (Planted Stands), PS-T (Planted Stands Thinned). Measurements include BA (Basal Area; m^2 ha^{-1}), AGB (Above Ground Biomass; Mg ha^{-1}), and CC (Crown Closure; %)

Stand Type	Parameter	Min	Max	Range	Mean	SD
NS	BA	16.1	48.2	60.4	36.5	9.1
PS	BA	11.5	52.8	41.3	25.6	15.0
PS-T	BA	11.5	25.3	13.8	17.9	3.7
NS	AGB	65.9	197.1	131.1	66.1	40.4
PS	AGB	79.3	262.3	182.9	132.5	69.7
PS–T	AGB	79.3	127.3	48.0	96.5	15.5
NS	CC	50.0	90.4	40.4	66.1	10.7
PS	CC	27.9	88.3	60.4	51.2	19.1
PS-T	CC	27.9	56.9	29.0	42.6	10.9

Table 3. Linear Regression Analysis for AGB (Above Ground Biomass) versus BA (Basal Area) and CC (Canopy Closure), and BA versus CC; Stand Types Correspond to NS (Natural Stands), PS (Planted Stands) and PS-T (Planted Stands Thinned)

Regression	Stand Type	R^2	p-value
AGB versus BA	NS	0.63	<0.01
AGB versus BA	PS	0.97	<0.01
AGB versus BA	PS-T	0.44	0.02
AGB versus CC	NS	0.18	0.20
AGB versus CC	PS	0.81	<0.01
AGB versus CC	PS-T	0.32	0.09
BA versus CC	NS	0.06	0.78
BA versus CC	PS	0.73	<0.01
BA versus CC	PS-T	0.07	0.46

to provide a quantificational comparison, the ubiquitously implemented Freeman decomposition was chosen as the method of choice. Upon initial inspection, the forested areas throughout the study area were primarily characterized by volumetric scattering (Plate 1). At each sample site, the classified pixels were extracted using a 5 × 5 window and the percentages of pixels dominated by each scattering type were calculated (Table 4). Volumetric scattering was dominant in all but three of 24 sites. After confirming our initial assumptions about the prevalence of volumetric scattering, we quantified scattering associated with the major cover types across the study area. We used the NLCD 2006 to identify the cover types associated with each pixel in the swath and associated the dominant scattering type to each. Volumetric scattering is shown to be prevalent in all forested cover classes (Table 5).

Correlation Analysis

Mean UAVSAR backscatter values were regressed against BA and AGB for the four sample groups (AS, NS, PS, and PS-T) at three window sizes (i.e., 3 × 3, 5 × 5, and 7 × 7 pixels) centered about the plot centers. All polarization combinations and pixel window sizes had relatively low correlation values compared with the *in situ* measurements of BA versus UAVSAR backscatter intensities. The mean HV and VV polarizations exhibited the strongest correlations across all four stand types and all three window sizes with the VV polarization displaying significantly better R^2 values within the PS-T stand type (R^2 = 0.41 to 0.48 (VV) versus R^2 = 0.00 to 0.20 (HV)) (Tables 6 and 7). With respect to optimal window size, the BA R^2 values generally trended upward as window size increased. The only anomalies were seen within the VV polarization where three of the four stand types (PS-T, NS, and AS) showed better correlations with the 5 × 5 window than that of the 7 × 7 (Tables 6 and 7). We expected the spatial averaging to generate a better estimate of the mean and reduce the variance provided that the spatial pattern remained homogeneous. However, these outliers are possibly a result of the vertical orientation of the target species lending to a higher interaction and attenuation in that particular polarization (Ramsey, 1998). The highest R^2 values for a particular stand type occurred within the PS stands across all three polarizations with the strongest correlation seen within the VV polarization's 7 × 7 window (R^2 = 0.74). Figure 2 shows the PS dominated R^2 value when compared to the other stand types.

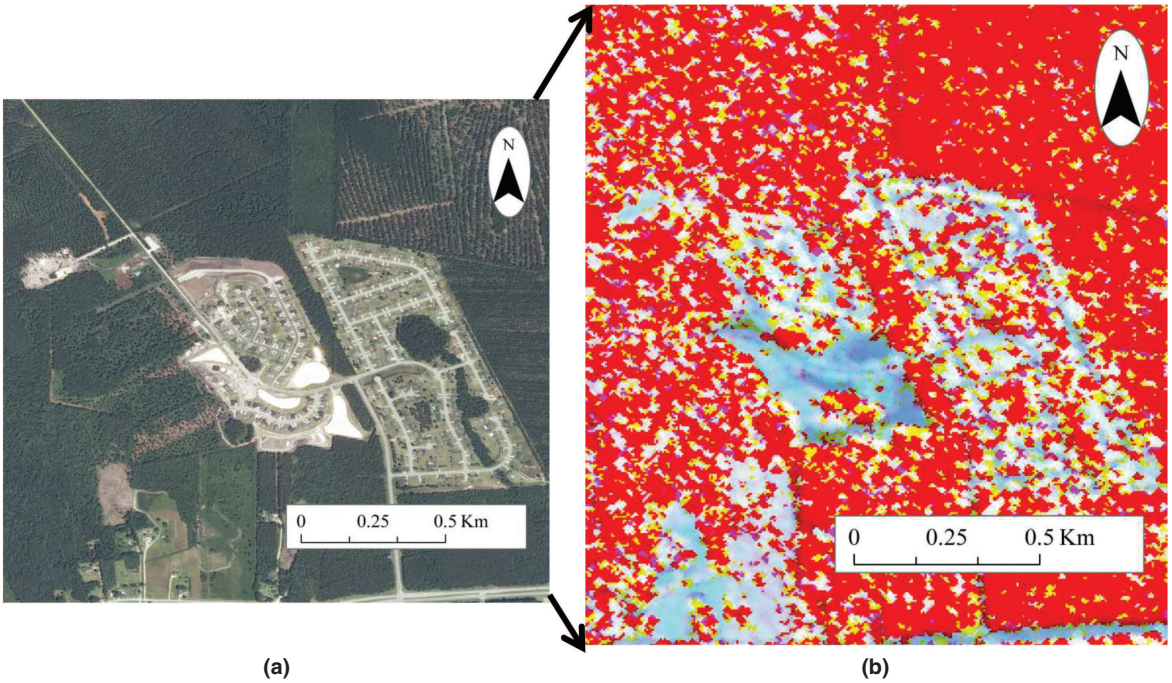

Plate 1. Representation of volumetric scattering for a subset of the UAVSAR data swath (a) in Carteret County, North Carolina as determined using the Freeman 3-component model. Volumetric scattering (b) dominated the forest class (red) and single bounce returns are indicative of open surfaces (blue-gray). The yellow-green areas are indicative of areas of single and double bounces, wetter areas with light vegetation prevalent.

Table 4. The Percentage of Pixels Dominated by Each Scattering Type across the 24 Sample Sites

Site	Single (%)	Double (%)	Volumetric (%)
1	92	0	8
2	8	0	92
3	4	0	96
4	60	0	40
5	0	0	100
6	0	0	100
7	0	0	100
8	0	0	100
9	0	0	100
10	0	0	100
11	0	0	100
12	0	0	100
13	0	0	100
14	0	0	100
15	0	0	100
16	0	0	100
17	0	0	100
18	20	0	80
19	28	0	72
20	20	0	80
21	8	0	92
22	0	0	100
23	0	0	100
24	80	12	8

Table 5. Scattering Type Occurrences for Each Major Cover Type within the Study Area

Landcover (NLCD 2006)	Single (%)	Double (%)	Volumetric (%)
Evergreen Forest	15.5	3.5	81.0
Deciduous Forest	22.0	3.4	74.5
Mixed Forest	18.1	3.1	78.8
Agriculture	71.1	7.9	21.0
Urban	41.0	16.9	42.1
Water	49.3	22.0	28.7
Wetland-woody	23.8	7.3	68.9
Wetland-emergent/ herbaceous	39.0	20.7	40.3
All cover types	42.2	8.8	49.0

Similar to the BA analysis, the mean AGB correlations with UAVSAR backscatter intensity for three of the four stand types (PS, NS, AS) showed the strongest R^2 values within the HV and VV polarizations (Tables 6 and 7). The HH polarization (R^2 = 0.16 to 0.38) showed the best fit for the PS-T stand, significantly outperforming the HV and VV correlation values (R^2 = 0.01 to 0.14) across the three window sizes. Similar to the BA correlation values, AGB correlation values increased with increasing window sizes for both the HH and HV polarizations; while the VV polarization correlation maximum was

Table 6. Regression Coefficients for 3 × 3, 5 × 5, and 7 × 7 Windows Comparing Loblolly Pine Above Ground Biomass (AGB) and Basal Area (BA) against the Mean Value HV Polarization; Note: *UF - unfiltered; F - filtered (median)

Parameter	Window	Stand Type	R^2 *(UF)/(F)	p–value *(UF)/(F)
AGB	3 × 3	PS	0.41/0.50	0.01/<0.01
AGB	3 × 3	PS-T	0.01/0.03	0.81/0.64
AGB	3 × 3	NS	0.51/0.52	0.01/<0.01
AGB	3 × 3	AS	0.27/0.33	0.01/<0.01
AGB	5 × 5	PS	0.50/0.53	0.01/<0.01
AGB	5 × 5	PS-T	0.02/0.04	0.69/0.59
AGB	5 × 5	NS	0.63/0.60	<0.01/0.01
AGB	5 × 5	AS	0.40/0.41	<0.01/<0.01
AGB	7 × 7	PS	0.59/0.59	<0.01/<0.01
AGB	7 × 7	PS-T	0.03/0.04	0.62/0.59
AGB	7 × 7	NS	0.55/0.53	0.01/0.01
AGB	7 × 7	AS	0.45/0.46	<0.01/<0.01
BA	3 × 3	PS	0.40/0.33	0.02/<0.01
BA	3 × 3	PS-T	0.00/0.08	0.90/0.43
BA	3 × 3	NS	0.11/0.11	0.32/0.31
BA	3 × 3	AS	0.06/0.09	0.26/0.15
BA	5 × 5	PS	0.55/0.58	<0.01/<0.01
BA	5 × 5	PS-T	0.13/0.17	0.31/0.24
BA	5 × 5	NS	0.15/0.18	0.23/0.21
BA	5 × 5	AS	0.14/0.15	0.07/0.06
BA	7 × 7	PS	0.65/0.68	<0.01/<0.01
BA	7 × 7	PS-T	0.20/0.26	0.20/0.13
BA	7 × 7	NS	0.18/0.16	0.19/0.23
BA	7 × 7	AS	0.21/0.22	0.03/0.02

at the 5 × 5 window size. The PS and NS stands exhibited the strongest correlations across all three polarizations with NS exhibiting the strongest correlations (Figure 3; Tables 6 and 7). Previously mature loblolly AGB has been partitioned into branches (26 percent), bole or main stem (38 percent) and needles (36 percent) (Chmura *et al.,* 2007). Thus, it was not surprising to see a better correspondence between NS and AGB due to more developed crown structure.

None of the three polarization derivatives (depolarization ratio, polarization correlation, and differential reflectivity ratio) that were also evaluated showed any significant correspondence to either AGB or BA.

Error Assessment

Numerous error sources may have negatively affected the coefficient of determination relationships between UAVSAR backscatter and forest density measurements. The first error source is the time differential between the radar and field data collection times. While it is unlikely that growth and other within stand changes (i.e., tree/limb loss due to storms, insects, disease, etc.) during the 18-month time interval caused a major reduction in performance, it is quite likely that some discrepancies were introduced. During this period, the growth rates between individual loblolly pine stands may have been differentially influenced by factors such as soil quality, possible insect infestations, stand age and density.

Table 7. Regression Coefficients for 3 × 3, 5 × 5, and 7 × 7 Windows Comparing Loblolly Pine Parameters (Para) (1) Above Ground Biomass (AGB) and (2) Basal Area (BA) against the Mean Value HV, HH, and VV Polarizations (POL); Note: (1) AGB RMSE = (Mg ha^{-1}), and (2) BA RMSE = (m^2 ha^{-1})

Para	Pol	Stand Type	3 × 3 R^2 /p–value/ RMSE*	5 × 5 R^2 /p–value/ RMSE*	7 × 7 R^2 /p–value/ RMSE*
AGB	HH	PS	0.23/0.10/58.95	0.32/0.04/55.22	0.42/0.02/51.22
AGB	HH	PS-T	0.16/0.25/13.44	0.33/0.08/12.00	0.38/0.06/11.58
AGB	HH	NS	0.41/0.03/32.14	0.40/0.04/32.13	0.33/0.07/34.35
AGB	HH	AS	0.19/0.03/51.42	0.24/0.02/49.91	0.25/0.01/49.43
AGB	VV	PS	0.41/0.02/51.31	0.58/<0.01/43.67	0.66/<0.01/38.98
AGB	VV	PS-T	0.14/0.29/13.62	0.07/0.45/14.11	0.08/0.43/14.07
AGB	VV	NS	0.58/0.01/27.28	0.63/<0.01/25.57	0.42/0.03/31.84
AGB	VV	AS	0.39/<0.01/44.54	0.49/<0.01/40.90	0.46/<0.01/42.17
AGB	HV	PS	0.41/0.01/47.16	0.50/0.01/45.77	0.59/<0.01/41.46
AGB	HV	PS-T	0.01/0.81/14.45	0.02/0.69/14.39	0.03/0.62/14.39
AGB	HV	NS	0.51/0.01/29.14	0.63/0.60/26.49	0.55/0.01/28.77
AGB	HV	AS	0.27/0.01/46.79	0.40/<0.01/44.07	0.45/<0.01/41.98
BA	HH	PS	0.23/0.09/12.61	0.34/0.04/11.69	0.45/0.01/10.71
BA	HH	PS-T	0.18/0.22/3.19	0.39/0.05/2.76	0.49/0.03/2.53
BA	HH	NS	0.05/0.52/8.46	0.03/0.61/8.54	0.04/0.54/8.48
BA	HH	AS	0.03/0.44/13.09	0.04/0.32/12.98	0.07/0.22/12.84
BA	VV	PS	0.49/0.01/10.33	0.67/<0.01/8.24	0.74/<0.01/7.35
BA	VV	PS-T	0.45/0.03/2.62	0.48/0.03/2.54	0.41/0.04/2.70
BA	VV	NS	0.20/0.17/7.77	0.18/0.19/8.17	0.16/0.25/8.01
BA	VV	AS	0.20/0.03/11.84	0.25/0.01/11.54	0.24/0.02/11.60
BA	HV	PS	0.40/0.02/9.91	0.55/<0.01/9.34	0.65/<0.01/8.10
BA	HV	PS-T	0.00/0.90/3.38	0.13/0.31/3.21	0.20/0.20/3.02
BA	HV	NS	0.11/0.32/8.17	0.15/0.23/7.91	0.18/0.19/7.93
BA	HV	AS	0.06/0.26/12.65	0.14/0.0712.23	0.21/0.03/11.74

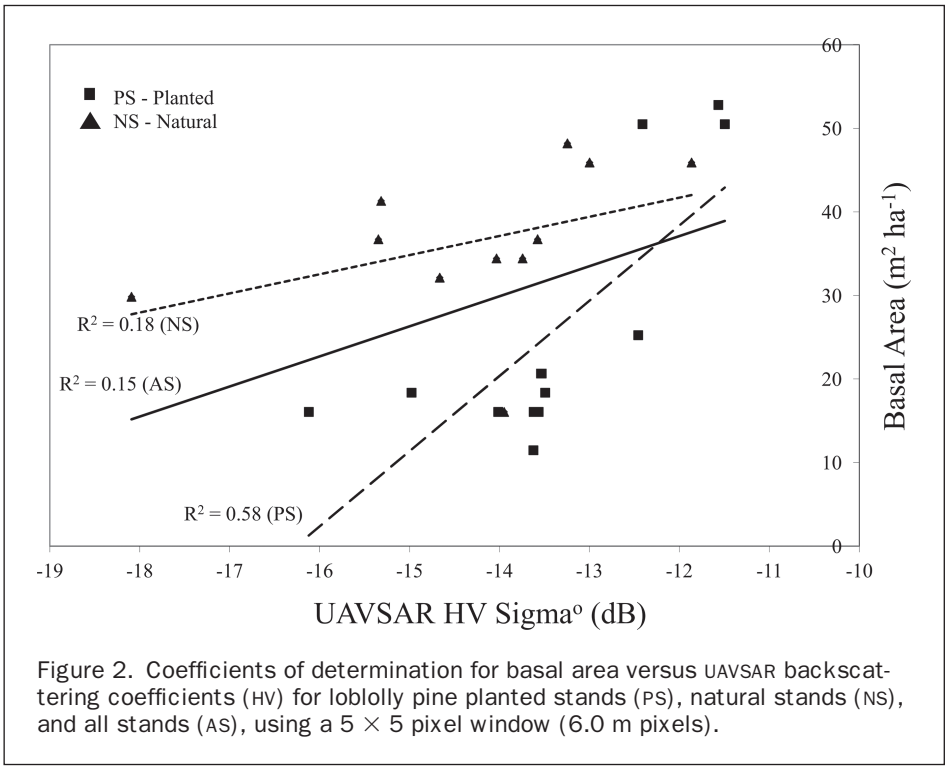

Figure 2. Coefficients of determination for basal area versus UAVSAR backscattering coefficients (HV) for loblolly pine planted stands (PS), natural stands (NS), and all stands (AS), using a 5 × 5 pixel window (6.0 m pixels).

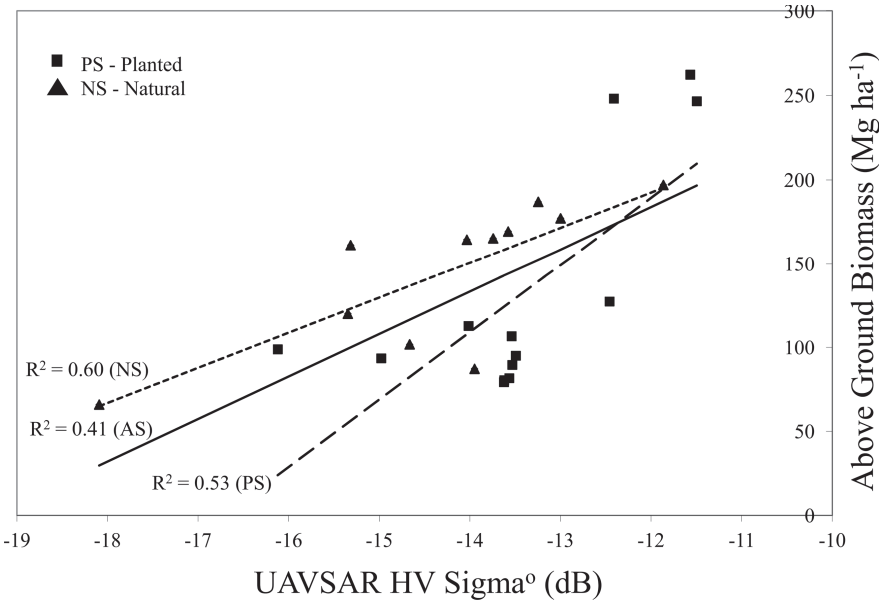

Figure 3. Coefficients of determination for ABG versus UAVSAR DB (HV) for loblolly pine stands planted (PS), natural (NS) and all (AS) using a 5 × 5 pixel window (6.0 m pixels).

It would be very difficult to determine the effect of these factors and apply them to this study. This is a problem inherent to many remote sensing studies, and likely had little impact. Another potential error source is associated with the inclusion of both natural and plantation pine stands in the AS sample population. Although limiting correlation analyses to a single type of stand in each analysis resulted in higher correlation values, the initial objective of the study was to determine the feasibility of inclusive modeling of all loblolly forests. With increasing forest complexity (i.e., NS, PS, and PS-T), the utility of L-band radar backscatter to predict BA and AGB decrease as reported in previous studies (Kasischke *et al.*, 1995). Additionally, variability was likely introduced from modeled values of AGB that were a function of the strength of the individual tree height versus DBH relationship established by Trincado *et al.* (2006).

The sensitivity of radar has been shown to decrease due to speckle noise (Saatchi *et al.,* 2011). Table 8 provides a summary of the HV backscatter intensity mean, standard deviation, and the coefficient of variation (CV) values found in the 3 × 3 pixel window size. The CV did not exceed the mean at any of the sites suggesting that the signal-to-noise ratio may have been reasonable for the data to be useful in its current state. To test this, a 9 × 9 pixel median filter was used to further smooth noise in the data. This did result in stronger correlations; however, these gains were small in magnitude (Table 6). The most substantial contributor to the weak correlations was likely the saturation of backscatter at a forest density threshold below the majority of the sample sites.

Other factors that require note include the wetness of the forest at the time of the data collect and the structural nature and distribution within this southern pine forest type. Moisture existent on the leaf surface at the time of the collect may limit the accuracy of foliage biomass estimates with radar (Sader, 1987). Dobson *et al.* (1991) found that numerous species (including pine) showed a backscatter change of 1 to 2 DB with L-band radar, primarily due to the increase in intercepted moisture in the tree crown. Much of the study the area received a significant amount of precipitation the day

Table 8. Within-stand HV Backscatter Intensity Variability (CV = Coefficient of Variation) for a 3 pixel × 3 pixel (18 m × 18 m) Window Surrounding Each Sample Site Center Point

Site	Stand Type	Mean	SD	CV
1	NS	−19.42	1.04	−0.05
2	NS	−15.82	1.35	−0.09
3	NS	−15.35	2.18	−0.14
4	PS/PS-T	−13.92	1.29	−0.09
5	PS/PS-T	−12.91	1.36	−0.11
6	PS/PS-T	−14.04	1.81	−0.13
7	PS	−12.52	1.37	−0.11
8	PS	−11.63	1.12	−0.10
9	PS	−12.61	1.73	−0.14
10	NS	−11.84	1.08	−0.09
11	NS	−13.32	0.38	−0.03
12	NS	−13.24	1.39	−0.11
13	NS	−13.49	1.96	−0.15
14	NS	−14.37	1.24	−0.09
15	PS/PS-T	−14.04	2.09	−0.15
16	PS/PS-T	−13.16	1.48	−0.11
17	PS/PS-T	−15.27	2.31	−0.15
18	NS	−13.94	2.06	−0.15
19	PS/PS-T	−12.97	2.04	−0.16
20	NS	−13.68	2.84	−0.21
21	NS	−13.82	2.03	−0.15
22	PS/PS-T	−13.76	2.18	−0.16
23	PS/PS-T	−12.59	1.77	−0.14
24	PS/PS-T	−15.23	1.68	−0.11

before the data collect. Even on the day of the collect, rain fell throughout the swath. It is unknown what effect the spatial distribution of the planted stands had on the double bounce returns received by the sensor. Weak correlations were seen between BA and AGB when compared to CC of the thinned pine. We do not believe that ground returns corrupted the biomass backscatter received by the antennae due to the milder look angle of all 24 plots (40° to 60.2°). Incidence angles less than 38° tend to capture ground surface returns, whereas the predominant returns near 60° tended to be canopy backscatter (Hoffer, 1986).

Study Comparisons

The overall utility of L-band radar for characterizing developed forests may be limited to regenerating stands (Dobson, 2000). As the canopies of loblolly pine stands surpass a certain density and AGB level, L-band energy is "largely attenuated by branches and needles" (Kasischke, *et al.*, 1995) rather than characterizing the large stems of individual trees which is necessary for estimating BA and AGB (Hussin, *et al.*, 1991). Double-bounce reflectance, in which the energy is not attenuated by the canopy, is the result of being reflected from the ground to the main stems (or vice versa) and returning to the antenna. This would likely be the ideal type of reflectance for characterizing BA.

Previous studies that have compared young open canopy low AGB stands with older dense high AGB stands have confirmed that L-band is more responsive under the former (Hussin, *et al.*, 1991; Kasischke, *et al.*, 1995; Stellingwerf and Hussin, 1997). The majority of the sites sampled in this study exceeded the 40 to 100 Mg ha^{-1} saturation range. The moderate correlations we encountered were congruent with the findings of Foody *et al.* (1997). In reporting the correlation coefficients of prior studies it is important to note that some higher R^2 values were attained by using forest stands within the dynamic range of biomass estimates, below the saturation levels (Rauste *et al.*, 1994; Dobson *et al.*, 1992). Further study under the environmental parameters encountered in this study will likely require the use of a longer wavelength SAR (P-band) to facilitate greater canopy penetration to increase double bounce returns.

Conclusions

The primary objective of this study was to explore the feasibility of using L-band radar to estimate BA and AGB of mature loblolly pine stands in the North Carolina coastal plain. We found correlations of determination ranging from weak (R^2 = 0.00 to 0.30) to moderate (R^2 = 0.30 to 0.70) for both BA and AGB measures ranging across the four stand types. The best correlations for the AGB versus UAVSAR backscatter were in the PS and NS stand types across all three polarizations. In contrast, the thinned pine stands exhibited the weakest correlations again across all three polarizations. HV and VV polarizations displayed the greatest sensitivity to AGB, consistent with other studies (Wu and Sader, 1987; Kasischke, *et al.*, 1995). The highest predictive capability for BA was seen in the PS and PS-T stand types using VV polarization.

The variability in the characteristics of mature plantation and natural loblolly pine stands lead to these poor-to-moderate correlations of determination. The study results suggested that BA and AGB can be more accurately measured when plantation and natural loblolly stands are modeled as separate groups. Accordingly, we concluded that the forest stands we measured likely exceeded the BA and AGB saturation thresholds for L-band radar. The prevalence of volumetric scattering at our sample sites upon the decomposition of the SAR also supported this conclusion.

The results from this research indicated that it is not feasible to accurately estimate BA and AGB of mature loblolly pine stands in the North Carolina coastal plain using simple linear regression with L-band radar DB, depolarization ratio, polarization correlation, and differential reflectivity ratio; particularly when natural and plantation stands are not analyzed independently. The high spatial resolution of the UAVSAR (6.0 m) provided no apparent improvement in performance compared to coarser resolution L-band SAR systems. Future research should be considered using longer wavelength P-band radar, due to the higher AGB saturation threshold. It may not be feasible to use L-band or shorter wavelength radar to measure these parameters in anything but young stands with lower BA and AGB found in this study. Furthermore, it is apparent that HV polarization should be focused on as it consistently displays the highest correlations with these types of forest measurements.

Acknowledgments

The authors would like to thank the three anonymous reviewers for their input into this work. Also, the authors would like to thank Dr. Elijah Ramsey for his feedback at various points along this process. The US Environmental Protection Agency funded and conducted the research described in this paper. It has been subject to the Agency's programmatic review and has been approved for publication. Mention of any trade names or commercial products does not constitute endorsement or recommendation for use.

References

Berni, J., P. Zarco-Tejada, L. Suarez, and E. Fererez, 2009. Thermal and narrow–band multispectral remote sensing for vegetation monitoring from an unmanned aerial vehicle, *IEEE Transactions on Geoscience and Remote Sensing*, 47:722–738.

Beyer, H.L. 2004. Hawth's Analysis Tools for ArcGIS, URL: *http://www.spatialecology.com/htools/* (last date accessed: 30 September 2013).

Chmura, D.J., M.S. Rahman, and M.G. Tjoelker, 2007. Crown structure and biomass allocation patterns modulate aboveground productivity in young loblolly pine and slash pine, *Forest Ecology and Management*, 243(1-2):219–230.

Coble, D.W., 2009. A new whole-stand model for unmanaged loblolly and slash pine plantations in east Texas, *Southern Journal of Applied Forestry*, 33(2):69–76.

Dandois, J.P., and E.C. Ellis, 2010. Remote sensing of vegetation structure using computer vision, *Remote Sensing*, 2(4): 1157-1176.

Dewey, J.C., S.D. Roberts, and I. Hartley, 2006. A comparison of tools for remotely estimating leaf area index in loblolly pine plantations, *Proceedings of the 13th Biennial Southern Silvicultural Research Conference* (K.F. Connor, editor), General Technical Report SRS-92, U.S. Department of Agriculture, Forest Service, Southern Research Station, Ashville, North Carolina, pp. 71–75.

Dobson, M.C., K. McDonald, F.T. Ulaby, and T. Sharik, 1991. Relating the temporal change observed by AIRSAR to surface and canopy properties of mixed conifer and hardwood forests of northern Michigan, *Proceedings of the 3rd Airborne Synthetic Aperture Radar (AIRSAR) Workshop* (J.J. van Zyl, editor), JPL Publication 91-30, Pasadena, California, pp. 34–43.

Dobson, M.C., F.T. Ulaby, T. LeToan, A. Beaudoin, E.S. Kasischke, and N. Christensen, 1992. Dependence of radar backscatter on coniferous forest biomass, *IEEE Transactions on Geoscience and Remote Sensing*, 30(2):412–415.

Dobson, M.C., 2000. Forest information from synthetic aperture radar, *Journal of Forestry*, 98(6):41–43.

ERDAS, 2010. ERDAS Field Guide 2010. URL: *http://geospatial.intergraph.com/fieldguide/wwhelp/wwhimpl/js/html/wwhelp.htm* (last date accessed: 30 September 2013).

Esri, 2013. ArcMap 10.1. Esri, Redlands, California.

European Space Agency (ESA): Polarimetric SAR Data Processing and Educational Tool (PolSARpro), 2012. URL: *http://envisat.esa.int/polsarpro/,* (last date accessed: 13 December 2012).

Foody, G.M., R.M. Green, R.M. Lucas, P.J. Curran, M. Honzak, and I.D. Amaral, 1997. Observations on the relationship between SIR-C radar backscatter and the biomass of regenerating tropical forests, *International Journal of Remote Sensing*, 18(3):687–974.

Franceschetti, G., and R. Lanari, 1999. *Synthetic Aperture Radar Processing*, Electronic Engineering Systems Series, CRC Press, 308 pp.

Freeman, A., and S.L. Durden, 1998. A three component model for polarimetric SAR data, *IEEE Transactions on Geoscience and Remote Sensing*, 36:963–973.

Hansch, R., 2010. Complex-valued multi-layer perceptions - An application to polarimetric SAR data, *Photogrammetric Engineering & Remote Sensing*, 76(9):1081–1088.

Hoffer, R., 1986. Analysis of multiple incidence angle SIR-B data for determining forest stand characteristics, *Proceedings of the 2nd Spaceborne Imaging Radar Symposium*, JPL, Pasadena, California 28-30 April.

Hussin, Y.A., R.M. Reich, and R.M. Hoffer, 1991. Estimating slash pine biomass using radar backscatter, *IEEE Transaction on Geoscience and Remote Sensing,* 29(3):427–431.

Iiames, J.S., R.G. Congalton, A.N. Pilant, and T.E. Lewis, 2008. Validation of an integrated estimation of Loblolly pine (*Pinus taeda l.*) leaf area index (LAI) utilizing two indirect optical methods in the southeastern United States, *Southern Journal of Applied Forestry*, 32(3):101–110.

Imhoff, M.L., 1993. *The Dependence of Synthetic Aperture Radar Backscatter on Forest Structure and Biomass: Potential Application for Global Carbon Models*, Ph.D. dissertation, Stanford University, Stanford, California, 280 p.

Imhoff, M.L., 1995. Radar backscatter and biomass saturation: Ramifications for global biomass inventory, *IEEE Transactions on Geoscience and Remote Sensing,* 33(2):511–518.

Imhoff, M.L., S. Carson, and P. Johnson, 1998. A low-frequency radar experiment for measuring vegetation biomass, *IEEE Transactions on Geoscience and Remote Sensing*, 36(6):1988–1991.

Jennings, S.B., N.D. Brown, and D. Sheil, 1999. Assessing forest canopies and understorey illumination: canopy closure, canopy cover and other measures, *Forestry*, 72(1):59–74.

Kasischke, E.S., N.L. Christensen, Jr., and L.L. Bourgeau-Chavez, 1995. Correlating radar backscatter with components of biomass in loblolly pine forests, *IEEE Transactions on Geoscience and Remote Sensing*, 33(3):643–659.

Lucas, R.M., A.K. Milne, N. Cronin, C. Witte, and R. Denham, 2000. The potential of synthetic aperture radar (SAR) for quantifying the biomass of Australia's woodlands, *Rangeland Journal*, 22(1):124–140.

McCoy, R.M., 2005. *Field Methods in Remote Sensing*, The Guilford Press, New York, 159 p.

Meyer, D., and L. Avery, 2009. Excel as a qualitative Data analysis tool, *Field Methods*, 21:91–112.

NASA JPL: Uninhabited aerial vehicle synthetic aperture radar, 2011. URL: *http://uavsar.jpl.nasa.gov/, National Aeronautics and Space Administration* (last date accessed: 30 September 2013).

North Carolina Forest Service (NCFS): Conserving working forest, North Carolina's Forest Resources Assessment: A statewide analysis of the past, current and projected future conditions of North Carolina's forest resources, 2010. URL: *http://www.ncforestassessment.com/PDF/NC%20Forest%20Assessment%20Complete.pd f* (last date accessed: 30 September 2013).

North Carolina OneMap: 2010 North Carolina NAIP Imagery, 2012. URL: *http://www.nconemap.com/* (last date accessed: 30 September 2013).

Orr, D.M., and A.W. Stuart, 2000. *The North Carolina Atlas: Portrait for a New Century*, The University of North Carolina Press, Chapel Hill, North Carolina, 480 p.

Ramsey III, E., 1998. Radar remote sensing of wetlands, *Remote Sensing Change Detection: Environmental Monitoring Methods and Applications* (R. Lunetta and C. Elvidge, editors), Ann Arbor Press, Inc., Chelsea, Michigan, pp. 211–243

Rauste, Y., T. Hame, J. Pulliainen, K. Heiska, and M. Hallikainen, 1994. Radar-based forest biomass estimation, *International Journal of Remote Sensing*, 15(14):2797–2808.

Robinson, C., S. Saatchi, M. Neumann, and T. Gillespie, 2013. Impacts of spatial variability on aboveground biomass estimation from L-band radar in a temperate forest, *Remote Sensing*, 5(3):1001–1023.

Rosen P.A., S. Hensley, K. Wheeler, G. Sadowy, and T. Miller, 2006. UAVSAR: A new NASA airborne SAR system for science and technology research, *Proceedings of the IEEE Conference on Radar*, Verona, New York, pp. 22–29.

Saatchi, S., M. Marlier, R.L. Chazdon, D.B. Clark, and A.E. Russell, 2011. Impact of spatial variability of tropical forest structure on radar estimation of aboveground biomass, *Remote Sensing of Environment,* 115(11):2836–2849.

Sader, S., 1987. Forest biomass, canopy structure, and species composition relationships with multipolarizalion L-band synthetic aperture radar data, *Photogrammetric Engineering & Remote Sensing*, 53(2):193–202.

Sampson, D.A., T.J. Albaugh, K.H. Johnsen, H.L. Allen, and S.J. Zarnoch, 2003. Monthly leaf area index estimates from point-in-time measurements and needle phenology for *Pinus taeda*, Canadian Journal Forest Research, 33:2477–2490.

Stellingwerf, D.A., and Y.A. Hussin, 1997. *Measurements and Estimations of Forest Stand Parameters Using Remote Sensing*, VSP, Utrecht, The Netherlands, 272 p.

Trincado, G., C.L. VanderSchaaf, and H.E. Burkhart, 2006. Regional mixed-effects height-diameter models for loblolly pine (*Pinus taeda L.*) plantations, *European Journal of Forest Research*, 126(2):253–262.

Wang, H., K. Ouchi., M. Watanabe, M. Shimada, T. Tadono, A. Rosenqvist, S.A. Romshoo, M. Matsuoka, T. Moriyama, and S. Uratsuka, 2006. In search of the statistical properties of high-resolution polarimetric SAR data for the measurements of forest biomass beyond the RCS saturation limits, *IEEE Geoscience and Remote Sensing Letters,* 3(4):495–499.

Waring, R.H., J.B. Way, E.R. Hunt, Jr., L. Morrissey, K.J. Ranson, J.F. Weishampel, R. Oren, and S.E. Franklin, 1995. Imaging radar for ecosystem studies, *BioScience*, 45(10):715–723.

Williams, T.M., and C.A. Gresham, 2006. Biomass accumulation in rapidly growing loblolly pine and sweetgum, *Biomass and Bioenergy*, 30(4):370–377.

Wu, S.T., 1987. Potential application of multipolarization SAR for pine-plantation biomass estimation, *IEEE Transactions on Geoscience and Remote Sensing,* GE-25(3):403–409.

Wu, S.T., and S.A. Sader, 1987. Multipolarization SAR data for surface feature delineation and forest vegetation characterization, *IEEE Transactions on Geoscience and Remote Sensing*, GE-25(1):67–76.

Zarco-Tejada, P.J., J.A.J. Berni, L. Suárez, G. Sepulcre-Cantó, F. Morales, and J.R. Miller, 2009. Imaging chlorophyll fluorescence from an airborne narrow-band multispectral camera for vegetation stress detection, *Remote Sensing of Environment*, 113:1262-1275.

(Received 23 January 2013; accepted 25 April 2013; final version 08 July 2013)